

Experimental and Computational Studies of Incorporation of Cyano Transition Metal Complexes in Potassium Chloride Crystals

D.J. Carter, M.I. Ogden and A.L Rohl.

Nanochemistry Research Institute, Curtin University of Technology, GPO Box U 1987, Perth WA 6845, Australia. M.Ogden@curtin.edu.au.

Abstract

Experimental and computational studies of the incorporation of hexacyanoferrate(II), hexacyanocobaltate(III), and hexacyanoferrate(III) into potassium chloride crystals are described. The experimental results showed that the extent of incorporation follows the trend, hexacyanoferrate(II) \gg hexacyanoferrate(III) $>$ hexacyanocobaltate(III). Computational modelling produced replacement energies that match the experimental trend. The calculated geometry of the incorporated complexes was also found to match well with previous experimental results.

Keywords: potassium chloride, molecular modelling, crystal growth, hexacyanoferrate, hexacyanocobaltate

Introduction

The incorporation of foreign molecules or ions in a growing crystal is a common phenomenon, despite the utility of crystallization as a purification method. Examples range from substitutions involving similar species, such as cation substitution in ionic solids, to systems where there is large disparity between the guest and the host lattice. Examples of the latter are often found in biomineralisation, where Nature achieves remarkable control of inorganic crystal growth, in part, by interaction with protein molecules.^[1] Attractive examples are found in the many ionic solids that have been found to incorporate dye molecules.^[2] Contamination of crystalline products is also of relevance to many industrial processes. Incorporation of impurities impacts on product quality, or complicates the disposal of by-products where, for example, toxic metals may be captured by otherwise innocuous materials.^[3]

One system of industrial significance is the doping of transition metal complexes into cubic halide crystals. In the production of salt by evaporation of saline water, hexacyanoferrate(II) is added to prevent caking.^[4] In the photographic industry,

transition metal complexes are incorporated into the silver halide microcrystals that comprise photographic emulsions, which mediate the formation of the latent image.^[5] Computer simulations of impurity incorporation in crystals should result in improved understanding of the crystal-additive interactions. Baetzold and coworkers have successfully used molecular modelling to probe the doping of both NaCl and AgCl with hexacyanoferrate(II) and hexacyanoferrate(III) using interatomic potentials^[6] and more recently have repeated the work on NaCl using embedded cluster calculations^[7], where the transition metal complex and the immediately surrounding lattice ions are simulated quantum mechanically whilst the rest of the lattice utilises interatomic potentials.

In this paper, we report experimental and computational results probing the incorporation of three additives, hexacyanoferrate(II), hexacyanocobaltate(III), and hexacyanoferrate(III) into potassium chloride. The work to date in the literature has probed the preferred environments of the transition metal complexes in the crystal lattice, rather than focus on how much can be adsorbed. We chose these three additives as although structurally similar, the first has a different charge to the other two, and they all have different metal–carbon bond lengths. Thus this series allows the effects of both charge and size on incorporation to be probed.

Results and Discussion

Crystal Growth

The aim of the experimental work was to determine the relative extent of incorporation of the three cyano complexes in potassium chloride crystals under slow growth conditions, for comparison with the computational results. A simple approach was taken where potassium chloride was crystallized in batches by controlled temperature reduction. The additive concentrations were varied from 10 ppm to 500 ppm, and the levels of incorporation determined by analysis of the metal content of the crystals. Hexacyanoferrate(II), hexacyanocobaltate(III), and hexacyanoferrate(III) were all found to incorporate into the crystal lattice. The results are summarised in Table 1. It is clear that the charge of the complex has a significant effect, with the iron(II) complex incorporated at levels an order of magnitude higher than the iron(III) and cobalt(III) complexes. The cobalt(III) complex is incorporated at levels consistently less than that of the iron(III) complex.

Incorporation of cyano complexes into potassium chloride has been reported previously with an emphasis on spectroscopic characterisation of the complex,^[8-12] and the effect of hexacyanoferrate(II/III) on the morphology of sodium chloride is well known with the iron(III) complex inducing a change from cubic to octahedral, and the iron(II) complex causing dendritic growth.^[4] It is interesting to note that in the present work, cubic crystals were produced in all cases. This may be a result of growing crystals by temperature reduction, rather than evaporation[†]; this observation requires further investigation but is outside the scope of the work presented here. To our knowledge, the extent of incorporation of these cyano complexes has not previously been reported under consistent experimental conditions.

Computational Modelling

To create space for a hexacyano complex in the KCl lattice, a KCl_6^{5-} moiety must first be removed. As the complexes have charges of -3 (hexacyanoferrate(III) and hexacyanocobaltate(III)) and -4 (hexacyanoferrate(II)), potassium vacancies surrounding the incorporated complex must also be introduced. The hexacyanoferrate(II) complex requires a single vacancy and the others two vacancies. These vacancies will be more stable the closer they are to the complex, but this requirement still leads to two possibilities for the single vacancy as shown in Figure 1 and nine possible divacancy configurations (see Figure 2).

To assess the thermodynamics of incorporating a hexacyano complex into a KCl crystal, the replacement energy is calculated:^[13]

$$E_{\text{replacement}} = (E_{\text{subs}} + nE_{\text{Cl}} + mE_{\text{K}} + nE_{\text{solv Cl}} + mE_{\text{solv K}}) - (E_{\text{cell}} + E_{\text{comp}} + E_{\text{solv comp}})$$

where E_{subs} is the lattice energy of the KCl cell with either $\text{Fe}(\text{CN})_6^{3-}$, $\text{Co}(\text{CN})_6^{3-}$ or $\text{Fe}(\text{CN})_6^{4-}$ substituted into it, E_{Cl} is the energy of an isolated chloride ion, E_{K} is the energy of an isolated potassium ion, $E_{\text{solv Cl}}$ is the energy of solvation of a chloride ion, $E_{\text{solv K}}$ is the energy of solvation of a potassium ion, E_{cell} is the energy of the KCl cell without the hexacyano complex, E_{comp} is the energy of $\text{Fe}(\text{CN})_6^{3-}$, $\text{Co}(\text{CN})_6^{3-}$ or

[†] Crystals of potassium chloride grown by evaporation of a drop of solution on a microscope slide did show changes in morphology consistent with the literature reports.

$\text{Fe}(\text{CN})_6^{4-}$ in a vacuum, $E_{\text{solv comp}}$ is the energy of solvation of $\text{Fe}(\text{CN})_6^{3-}$, $\text{Co}(\text{CN})_6^{3-}$ or $\text{Fe}(\text{CN})_6^{4-}$, n is the number of chloride ions removed from the lattice to accommodate the complex and finally m is the number of potassium ions removed. The lattice energies and energies of the isolated ions were calculated using the GULP code^[14] utilizing the potentials and partial atomic charges discussed in the Experimental section. A 3x3x3 supercell of KCl was used to keep the periodic repeating incorporated complexes from interacting with each other to any significant extent. The solvation energies were calculated as reported previously^[13].

Tables 2 and 3 list the calculated replacement energies for the three different complexes in KCl. The hexacyanoferrate(II) vacancies are more stable (lowest energy) than the hexacyanoferrate(III) or hexacyanocobaltate(III) divacancies, with the 101 configuration producing the most stable configuration of all. For hexacyanoferrate(III) and hexacyanocobaltate(III), the order of most stable to least stable divacancies is the same. The hexacyanoferrate(III) complex is more stable for the two most stable divacancy configurations than the equivalent hexacyanocobaltate(III) configuration. Remarkably, for the rest the order of stability is reversed. The most stable divacancy configuration is the $110 \bar{1} \bar{1} 0$ and the least stable configuration is the $200 \bar{2} 00$ configuration. It should be noted that the energy differences between the $110 \bar{1} \bar{1} 0$ and $\bar{1} \bar{1} 0 101$ divacancy configurations of hexacyanoferrate(III) and hexacyanocobaltate(III) are all less than RT, suggesting that all four are equally likely at room temperature. Baetzold^[6] performed similar defect calculations examining the incorporation of hexacyanoferrate(III) in sodium chloride. He also found that the $110 \bar{1} \bar{1} 0$ configuration was the most stable but with the next stable $\bar{1} \bar{1} 0 101$ configuration within RT. Electron paramagnetic resonance (EPR) spectra measured by Wang, Meijers and de Boer^[12] demonstrates that the $110 \bar{1} \bar{1} 0$ configuration is the most stable in both sodium and potassium chloride, followed by $\bar{1} \bar{1} 0 101$. Thus although the interatomic potentials are not producing quantitative energy differences between configurations, they are giving a qualitatively correct description of the relative stabilities within these systems.

It is tempting to try and explain the replacement energy trends in terms of charge matching and lattice fit. To maintain charge neutrality with hexacyanoferrate(II), only one cation vacancy is required. Hexacyanoferrate(III) and hexacyanocobaltate(III)

require two cation vacancies. Energy is required to create these cation vacancies, so fewer vacancies will be energetically favorable. This is why the replacement energies for hexacyanoferrate(II) are the lowest. This correlates well with the experimental data, with hexacyanoferrate(II) incorporating to the greater extent. Hexacyanocobaltate(III) and hexacyanoferrate(III) have the same charge, so the difference in replacement energies could be related to the lattice fit. The Cl-K-Cl distance (including the ionic radius of chlorine) for potassium chloride is 9.92 Å. The linear distance across N-C-M-C-N (including the van der Waals radius of nitrogen), where M represents Fe^{3+} and Co^{3+} , is 9.47 Å and 9.39 Å respectively. This suggests that the best match is with hexacyanoferrate(III) and thus it should incorporate preferentially over hexacyanocobaltate(III). This agrees with the experimental data reported herein and the two calculated lowest energy configurations, but not for the less stable possibilities. This strongly suggests that even at the higher dosages, most of the hexacyanoferrate(III) and hexacyanocobaltate(III) ions are incorporating with the two most stable divacancies. These results show that while simple geometric considerations can provide a preliminary guide to additive-crystal interactions, more detailed studies are required for accurate explanations and predictions. In this case, it would appear that the charge distribution (which varies significantly between $\text{Fe}(\text{CN})_6^{3-}$ and $\text{Co}(\text{CN})_6^{3-}$) is an important factor in determining the replacement energies, and can compensate for differences in fit.

Another important result that can be obtained from molecular modelling calculations is the geometry of the minimised configurations. For hexacyanoferrate(III) with the most stable divacancy configuration, the cyano ligands are calculated to distort by 7.7° from octahedral as shown in Figure 3. Experimental EPR measurements by Wang, Meijers and de Hoer^[12] showed distortions from octahedral symmetry of 6-8°. This close agreement with experimental results suggests that the interatomic potentials derived in this work are of high quality. The distortions for the hexacyanocobaltate(III) with the same defect configuration is 7.2° and for hexacyanoferrate(II) with its most stable defect is 4.8°. The hexacyanoferrate(II) presumably distorts to a lesser extent than the other complexes because there is only one vacancy in the supercell.

Conclusion

A new set of interatomic potentials for hexacyano complexes has been developed, and utilised in the modelling of the incorporation of these complexes in the potassium chloride lattice. The results obtained were consistent with experimental data in terms of both levels of incorporation and geometry of the complexes within the crystal.

Experimental

Materials

Potassium chloride and potassium hexacyanoferrate(II) (AR grade) were supplied by Ajax Chemicals. Potassium hexacyanocobaltate(III) and potassium hexacyanoferrate(III) (AR grade) were supplied by the Aldrich Chemical Company.

Crystal Growth

Solutions of potassium chloride (5.9 M, supersaturation ratio of 1.13 at 30 °C) with varying levels of additive, were prepared. Additive concentrations used were 10, 50, 100, 250 and 500 ppm. Each solution (including blanks) was heated to approximately 80°C and filtered hot through a Gelman 0.2 µm membrane filter before being placed in a rotating waterbath. The temperature was held at 80°C for approximately 90 minutes and then ramped down from 80°C to 30°C, at a rate of 5 mins/°C. The temperature was then held at 30°C for several hours. The crystals were isolated by filtration and washed with a sequence of saturated potassium chloride solutions containing increasing amounts of ethanol. Some samples were crushed and rewashed before analysis to ensure macro-inclusions in the crystal were not biasing results. No significant changes in metal concentration were observed. Additive levels were determined by atomic absorption spectroscopy.

Generation of potential model

As the incorporation of hexacyanocobaltate(III) ions into any ionic lattice has not been previously modeled, we took the opportunity to develop a new set of interatomic potentials for hexacyano complexes. The charges on the atoms in each complex were calculated using the charge equilibration process of Rappe and Goddard.^[15] For the three complexes, a potential energy hypersurface was constructed with the density functional techniques built into the DMol^[16] program using the DNP basis set^[17] and BLYP functional^[18, 19]. Two and three body potential functions describing all the

internal degrees of freedom for each complex were fitted to the relevant hypersurface using the GULP code^[14]. The two body interactions were described using a harmonic potential:

$$E_{ij} = \frac{1}{2}k(r_{ij}-r_o)^2$$

where k is the spring constant, r_o is the equilibrium bond length constant and r_{ij} is the actual length. A cosine potential function was utilized to describe the three body interactions:

$$E_{ijk} = k(-\cos(n\theta_{ijk}) + 1)$$

where k is the three body constant, θ_{ijk} is the bond angle and n is the periodicity.

The van der Waals parameters for the atoms in the complex as well as the K^+ and Cl^- ions were taken from the ESFF force field,^[20] using the Lennard Jones 9-6 potential described below:

$$E_{ij} = \overset{\circ}{a}_{ij} \left[2 \left(\frac{r_{ij}^*}{r_{ij}} \right)^9 - 3 \left(\frac{r_{ij}^*}{r_{ij}} \right)^6 \right]$$

where $\overset{\circ}{a}_{ij}$ is the potential well depth and r_{ij}^* is the interatomic distance at which the maximum occurs.

Polarisation of the chlorine ions was incorporated via the shell model of Catlow, Diller and Norbett^[21]. In this model, a massless shell is connected via a spring to the core. The total charge is distributed across the core and shell, thus polarization occurs when they separate. The spring is harmonic:

$$E_i = \frac{1}{2} k r_i^2$$

where r_i is the core/shell separation. These parameters are summarized in Table 4.

References

- [1] E. Baeuerlein (eds.), *Biomineralization*, Wiley-VCH, Weinheim, 2000.
- [2] B. Kahr and R. W. Gurney, *Chem. Rev.*, **2001**, *101*, 893.
- [3] C. Koopman, C. J. Witkamp and G. M. Van Rosmalen, *Sep. Sci. Technol.*, **1999**, *34*, 2997.
- [4] M. A. H. Behrens, R. Lacmann and W. Schroeder, *Chem. Eng. Technol.*, **1995**, *18*, 295.
- [5] M. T. Bennebroek, J. Schmidt, R. S. Eachus and M. T. Olm, *J. Phys.: Condens. Matter*, **1997**, *9*, 3227.
- [6] R. C. Baetzold, *J. Phys. Chem. B*, **1997**, *101*, 1130.
- [7] P. V. Sushko, A. L. Shluger, R. C. Baetzold and C. R. A. Catlow, *J. Phys.: Condens. Matter*, **2000**, *12*, 8257.
- [8] S. C. Jain, A. V. R. Warriar and H. K. Sehgal, *J. Phys. C*, **1972**, *5*, 1511.
- [9] S. C. Jain, A. V. R. Warriar and H. K. Sehgal, *J. Phys. C*, **1973**, *6*, 193.
- [10] A. K. Viswanath and M. T. Rogers, *J. Chem. Phys.*, **1981**, *75*, 4183.
- [11] D. M. Wang, G. E. Janssen, S. M. Meijers, A. A. K. Klaassen and E. De Boer, *Bull. Magn. Reson.*, **1989**, *11*, 379.
- [12] D. M. Wang, S. M. Meijers and E. De Boer, *Mol. Phys.*, **1990**, *70*, 1135.
- [13] A. L. Rohl, D. H. Gay, R. J. Davey and C. R. A. Catlow, *J. Am. Chem. Soc.*, **1996**, *118*, 642.
- [14] J. D. Gale, *J. Chem. Soc., Faraday Trans.*, **1997**, *93*, 629.
- [15] A. K. Rappè and W. A. Goddard, *J. Phys. Chem.*, **1991**, *95*, 3358.
- [16] DMol Version 960, Accelrys, 1996.
- [17] B. J. Delley, *J. Chem. Phys.*, **1990**, 508.
- [18] C. Lee, W. Yang and R. G. Parr, *Phys. Rev. B*, **1988**, *37*, 785.
- [19] A. D. Becke, *Phys. Rev. A*, **1988**, *38*, 3098.
- [20] S. Barlow, A. L. Rohl, S. G. Shi, C. M. Freeman and D. O'Hare, *J. Am. Chem. Soc.*, **1996**, *118*, 7578.
- [21] C. R. A. Catlow, K. M. Diller and M. J. Norgett, *J. Phys. C: Solid State Phys.*, **1977**, *10*, 1395.

Table 1. Experimentally determined incorporation of hexacyanoferrate(II), hexacyanocobaltate(III), and hexacyanoferrate(III) into KCl.

Initial additive concentration (ppm)	Concentration of complex in KCl (mg/g)		
	$K_4Fe(CN)_6$	$K_3Fe(CN)_6$	$K_3Co(CN)_6$
10	0.11±0.01	0.05±0.01	0.03±0.01
50	0.61±0.06	0.09±0.01	0.05±0.01
100	1.17±0.12	0.11±0.01	0.07±0.01
250	2.87±0.29	0.25±0.02	0.12±0.01
500	3.71±0.37	0.35±0.03	0.28±0.03

Table 2. The energy differences for replacing KCl_6^{5-} and associated vacancies with $Fe(CN)_6^{3-}$ and $Co(CN)_6^{3-}$, compared to the most stable vacancy. For the $110 \bar{1} \bar{1} 0$ defect with $K_3Fe(CN)_6$ the replacement energy was -2368.68 kJ/mol.

DEFECT	$\Delta E_{\text{replacement}}$ (kJ/mol)	
	$K_3Fe(CN)_6$	$K_3Co(CN)_6$
$110 \bar{1} \bar{1} 0$	0.00	0.91
$\bar{1} \bar{1} 0 101$	0.97	1.09
$\bar{1} 0 \bar{1} 10 \bar{1}$	22.68	19.13
$\bar{1} 01 0 \bar{1} 1$	22.87	21.89
$110 200$	29.74	27.50
$011 200$	36.29	33.52
$\bar{1} \bar{1} 0 200$	41.83	39.89
$\bar{2} 00 020$	72.21	67.49
$200 \bar{2} 00$	109.46	104.48

Table 3. The energy differences for replacing KCl_6^{5-} and associated vacancies with $\text{Fe}(\text{CN})_6^{4-}$, compared to the most stable vacancy. For the 101 defect in $\text{K}_4\text{Fe}(\text{CN})_6$ and the replacement energy was -3744.30 kJ/mol.

	$\Delta E_{\text{replacement}}$ (kJ/mol)
DEFECT	$\text{K}_4\text{Fe}(\text{CN})_6$
101	0.00
200	27.32

Table 4. Potential parameters used in this work.

<i>Harmonic potentials</i>		k (eV/Å ²)	r_0 (Å)		
Ferrocyanide	Fe ²⁺ -C	6.4961	2.0029		
	C-N	89.7062	1.2047		
Ferricyanide	Fe ³⁺ -C	8.4069	1.9928		
	C-N	96.6837	1.1933		
Cobalticyanide	Co ³⁺ -C	8.8578	1.9566		
	C-N	97.1404	1.1905		
<i>3-Body Potentials</i>		k (eV)	θ_0 (°)	n	
Ferrocyanide	Fe ²⁺ -C-N	0.6451	180	2	
	C-Fe ²⁺ -C	0.2352	90	4	
Ferricyanide	Fe ³⁺ -C-N	0.5229	180	2	
	C-Fe ³⁺ -C	0.1839	90	4	
Cobalticyanide	Co ³⁺ -C-N	0.5452	180	2	
	C-Co ³⁺ -C	0.2274	90	4	
<i>Lennard Jones potentials</i>		ϵ_{ij} (eV)	r_{ij}^* (Å)		
Ferrocyanide	K	0.02428	3.1229		
	Cl	0.00292	5.2249		
	Fe ²⁺	0.01348	3.6769		
	C	0.00209	3.9559		
Ferricyanide	N	0.00211	3.8072		
	Fe ³⁺	0.01755	3.3708		
	C	0.00235	3.8983		
Cobalticyanide	N	0.00211	3.8072		
	Co ³⁺	0.01810	3.3460		
	C	0.00237	3.8947		
	N	0.00211	3.8072		
<i>Charges</i>					
Ferrocyanide	K	1.0000			
	Cl _{core}	1.4850			
	Cl _{shell}	-2.4850			
	Fe ²⁺	0.9938			
Ferricyanide	C	-0.2697			
	N	-0.5626			
	Fe ³⁺	1.0549			
Cobalticyanide	C	-0.1297			
	N	-0.5461			
	Co ³⁺	0.9999			
	C	-0.1214			
	N	-0.5453			
<i>Shell Model</i>		k (eV/Å ²)			
	Cl	29.38			

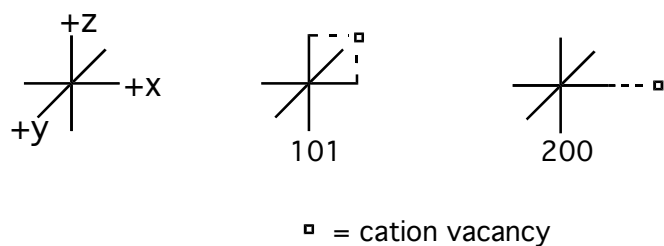


Figure 1. The two possible cation vacancy configurations when $\text{Fe}(\text{CN})_6^{4-}$ is substituted into potassium chloride.

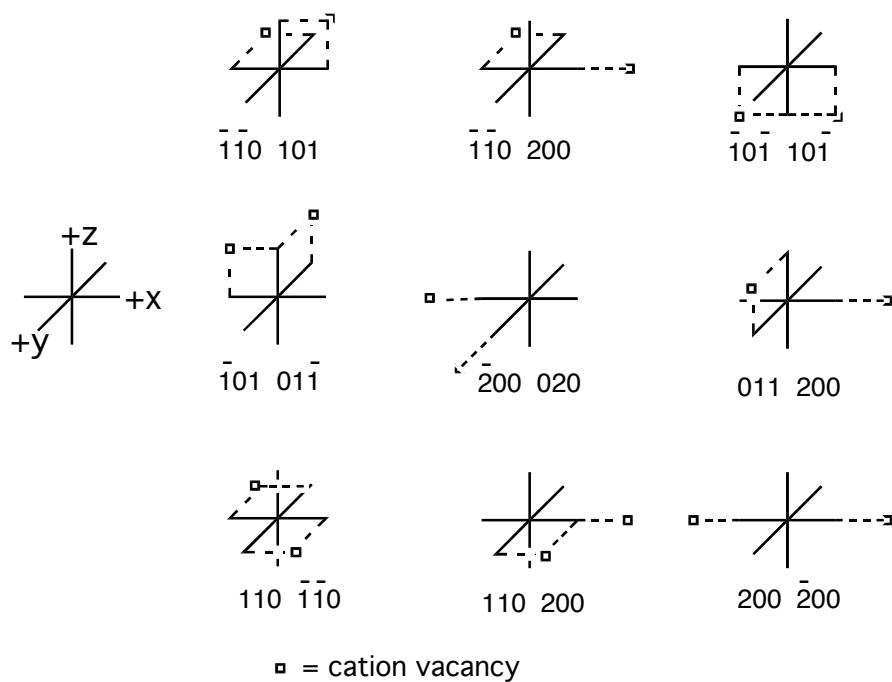


Figure 2. The nine possible divacancy configurations when $\text{Fe}(\text{CN})_6^{3-}$ or $\text{Co}(\text{CN})_6^{3-}$ are substituted into potassium chloride.

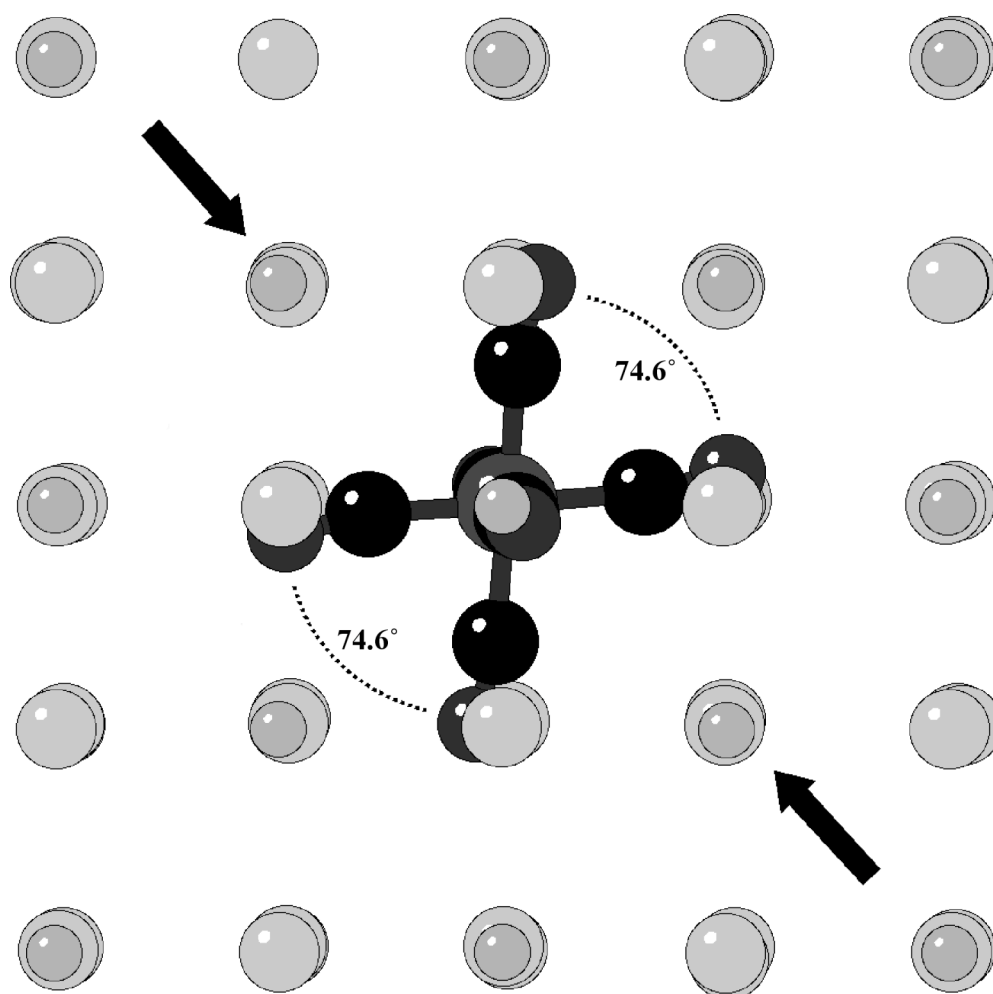
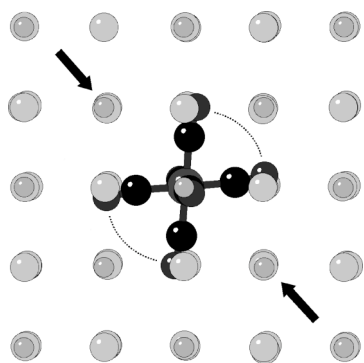


Figure 3. View along the z direction showing distortion of the cyanide ligands from octahedral when $\text{Fe}(\text{CN})_6^{3-}$ is relaxed within KCl, in the presence of 110 and $\bar{1}\bar{1}0$ defects (indicated by arrows).

Graphical Abstract



Experimental and computational studies of the incorporation of hexacyanoferrate(II), hexacyanocobaltate(III), and hexacyanoferrate(III) complex anions into potassium chloride crystals are described. The extent of incorporation follows the trend, hexacyanoferrate(II) \gg hexacyanoferrate(III) $>$ hexacyanocobaltate(III). Computational modelling produced replacement energies and geometries that match the experimental results.